Unique Barium Selenostannate−Selenide: $Ba_7Sn_3Se_{13}$ (and Its Variants $Ba_7Sn_3Se_{13-\delta}Te_\delta$) with $SnSe_4$ Tetrahedra and Isolated Se Anions

Abdeljalil Assoud and Holger Kleinke*

Department of Chemistry, University of Waterloo, Waterloo Ontario N2L 3G1

Received April 13, 2005. Revised Manuscript Received May 24, 2005

The new selenostannate−selenide $Ba_7Sn_3Se_{13}$ and its quaternary substitution variants $Ba_7Sn_3Se_{13-\delta}Te_\delta$ were prepared from the elements at 900 °C followed by slow cooling to 200 °C. $Ba_7Sn_3Se_{13}$ crystallizes in the orthorhombic space group *Pnma*, with lattice parameters of $a = 12.748(1)$ Å, $b = 24.891(3)$ Å, $c = 9.212(1)$ Å, and $V = 2923.0(5)$ Å^3 ($Z = 4$). The structure motifs include Ba^{2+} cations, isolated $SnSe_4$ tetrahedra, and isolated Se^{2-} anions that are not bonded to any Sn atom. Partial Se/Te replacements are possible up to 2.24(2) of the 13 Se atoms, and the Te atoms prefer the naked site, surrounded by six Ba^{2+} cations, as well as the site with the longest Se−Ba distances. The Se/Te substitution leads to a smaller band gap as computed with the LMTO approximation, which becomes visible by the gradual darkening of the red color with increasing Te content.

Introduction

The thermoelectric materials research area is currently receiving renewed interest, thereby revealing a number of materials in part superior to the commercial ones.[1−5] It is generally accepted knowledge that thermoelectric materials are narrow gap semiconductors with heavy constituent elements.[6,7] Among others, Zintl phases may be of particular interest. Recently, we uncovered two new Sr seleno−stannates, Sr_2SnSe_5 with polyselenide groups and $SrSn_2Se_4$ with mixed valent Sn atoms, exhibiting calculated band gaps of 0.9 and 0.2 eV, respectively,[8] and a new Ba_2SnTe_5 modification with a gap of around 0.2 eV (calculated and confirmed experimentally).[9]

It was interesting to realize that several of the most simple seleno−stannates A_2SnSe_4 (A = Sr, Ba), comprising A^{2+} cations and isolated $SnSe_4$ tetrahedra, are not discovered yet, while among the thio−stannates, Sr_2SnS_4[10] and two Ba_2SnS_4 modifications[11,12] are published. Such materials would be important reference points for studies of the changes arising from the polyselenide groups and/or mixed valent Sn atoms. During our attempts to synthesize the elusive Ba_2SnSe_4, we discovered $Ba_7Sn_3Se_{13}$ with the most common oxidation states (+2 for Ba, +4 for Sn, and −2 for Se). $Ba_7Sn_3Se_{13}$ forms a unique structure that is being introduced with this contribution, together with its substitution variants $Ba_7Sn_3Se_{13-\delta}Te_\delta$.

Experimental Procedures

Synthesis. All reactions started from the elements (Ba: 99% nominal purity, pieces, Aldrich; Sn: 99.8%, powder −325 mesh, ALFA AESAR; Se: 99.8%, powder −200 mesh, Aldrich; and Te: 99.8%, powder, −200 mesh, Aldrich), with a total sample mass of around 500 mg. We first encountered $Ba_7Sn_3Se_{13}$ by heating the elements Ba, Sn, and Se in the 2:1:4 ratio in an evacuated silica tube to 900 °C, followed by slow cooling to 200 °C within 5 days. After its successful characterization via an X-ray single-crystal structure study, we repeated that reaction starting from the stoichiometric ratio. Moreover, we tried to replace Se with Te to various extents, up to a starting Se/Te ratio of 5:8 using the same reaction conditions.

Analyses. Phase identifications were carried out by powder X-ray diffractometry (using an INEL diffractometer with position-sensitive detector and $CuK\alpha_1$ radiation) from the ground products in all cases. Starting at an Se/Te ratio of 10:3, the formation of binary tellurides as side products became evident. Selected crystals were analyzed by means of standardless energy dispersive spectroscopy (EDS, LEO 1530, with integrated EDAX Pegasus 1200) using an acceleration voltage of 21 kV, a procedure that verified the existence of the desired elements within the products, and most importantly an increasing Te content with increasing Te starting amounts. No

* To whom correspondence should be addressed. E-mail: kleinke@uwaterloo.ca.

(1) Sales, B. C.; Mandrus, D.; Williams, R. K. *Science* **1996**, *272*, 1325−1328.
(2) Chung, D.-Y.; Hogan, T.; Brazis, P.; Rocci-Lane, M.; Kannewurf, C.; Bastea, M.; Uher, C.; Kanatzidis, M. G. *Science* **2000**, *287*, 1024−1027.
(3) Venkatasubramanian, R.; Slivola, E.; Colpitts, T.; O'Quinn, B. *Nature* **2001**, *413*, 597−602.
(4) Hsu, K. F.; Loo, S.; Guo, F.; Chen, W.; Dyck, J. S.; Uher, C.; Hogan, T.; Polychroniadis, E. K.; Kanatzidis, M. G. *Science* **2004**, *303*, 818−821.
(5) Chung, D.-Y.; Hogan, T. P.; Rocci-Lane, M.; Brazis, P.; Ireland, J. R.; Kannewurf, C. R.; Bastea, M.; Uher, C.; Kanatzidis, M. G. *J. Am. Chem. Soc.* **2004**, *126*, 6414−6428.
(6) Rowe, D. M. *CRC Handbook of Thermoelectrics*; CRC Press: Boca Raton, FL, 1995.
(7) DiSalvo, F. J. *Science* **1999**, *285*, 703−706.
(8) Assoud, A.; Soheilnia, N.; Kleinke, H. *Chem. Mater.* **2004**, *16*, 2215−2221.
(9) Assoud, A.; Derakhshan, S.; Soheilnia, N.; Kleinke, H. *Chem. Mater.* **2004**, *16*, 4193−4198.
(10) Pocha, R.; Tampier, M.; Hoffmann, R.-D.; Mosel, B. D.; Pöttgen, R.; Johrendt, D. *Z. Anorg. Allg. Chem.* **2003**, *629*, 1379−1384.
(11) Jumas, J. C.; Philippot, E.; Vermot-Gaud-Daniel, F.; Ribes, M.; Maurin, M. *J. Solid State Chem.* **1975**, *14*, 319−327.
(12) Susa, K.; Steinfink, H. *J. Solid State Chem.* **1971**, *3*, 75−82.

10.1021/cm050787y CCC: $30.25
Published on Web 07/27/2005

Table 1. Crystallographic Data for $Ba_7Sn_3Se_{13-\delta}Te_\delta$

chemical formula	$Ba_7Sn_3Se_{13}$	$Ba_7Sn_3Se_{11.90(3)}Te_{1.10}$	$Ba_7Sn_3Se_{11.24(2)}Te_{1.76}$	$Ba_7Sn_3Se_{10.76(2)}Te_{2.24}$
formula weight [g/mol]	2343.93	2397.43	2429.29	2453.13
T of measurement [K]	298(2)	298(2)	298(2)	298(2)
λ [Å]	0.71073	0.71073	0.71073	0.71073
space group	*Pnma*	*Pnma*	*Pnma*	*Pnma*
a [Å]	12.748(1)	12.845(3)	12.9244(6)	12.9596(6)
b [Å]	24.891(3)	25.098(6)	25.183(1)	25.242(1)
c [Å]	9.212(1)	9.242(2)	9.2746(4)	9.2920(4)
V [Å^3]	2923.0(5)	2980(1)	3018.7(2)	3039.6(2)
Z	4	4	4	4
μ [mm-^{1}]	27.959	27.140	26.619	26.310
ρ_{calcd} [g/cm^3]	5.326	5.344	5.345	5.361
$R(F_o)^a\backslash R_w(F_o^2)^b$	0.0535\0.0923	0.0442\0.0847	0.0292\0.0583	0.0333\0.0663

[a] $R(F_o) = \Sigma||F_o| - |F_c||/\Sigma|F_o|$. [b] $R_w(F_o^2) = [\Sigma[w(F_o^2 - F_c^2)^2]/\Sigma[w(F_o^2)^2]\ ]^{1/2}$.

heteroelements (e.g., stemming from the reaction container) were found in any case.

Single-Crystal Structures. The data collections were carried out on a BRUKER Smart Apex CCD at room temperature utilizing MoKα radiation. The crystals were picked from four different reactions, namely, from the first reaction aiming at Ba_2SnSe_4 and from three reactions designed to determine the phase range of $Ba_7Sn_3Se_{13-\delta}Te_\delta$, with Se/Te ratios of 10:3, 1:1, and 5:8. Data were collected by scans of 0.3° in ω in at least two blocks of 606 frames at $\phi = 0$ and 120°, with exposure times of 30−40 s per frame for all four cases. The data were corrected for Lorentz and polarization effects, and absorption corrections were based on fitting a function to the empirical transmission surface as sampled by multiple equivalent measurements[13] since the crystal faces could not be determined reliably for numerical absorption corrections. Structure solution and refinements were performed with the SHELXTL package.[14]

Orthorhombic symmetry was expected based on the cell dimensions in each case, and the systematic absences restricted the possible space groups to *Pnma* and $Pna2_1$. We utilized the Direct Methods to locate the atomic positions in *Pnma* in the case of the ternary selenide. The assignment of four Ba, two Sn, and eight Se atoms to these positions was straightforward, and the refinements against F^2 converged with a residual factor of $R_w(F_o^2) = 0.092$. In the cases of the selenide−tellurides, we first refined all chalcogen sites as Se, which lead to unreasonably small displacement parameters of Se7 and Se8. In the next step, these two sites, called Q7 and Q8, were refined as mixed occupied Se/Te positions. This resulted in significant Se/Te mixing in all cases, ranging from 23.3(6) to 70.5(11)% Se. Next, each Se site (i.e., Se1 to Se6, one after the other) was as well treated like an Se/Te mixed position. However, no Te contents larger than twice the value of the standard deviation were observed. Therefore, we fixed the occupancies for the sites Se1 to Se6 at 100% Se each. This resulted in refined formulas of $Ba_7Sn_3Se_{11.90(3)}Te_{1.10}$, $Ba_7Sn_3Se_{11.24(2)}Te_{1.76}$, and $Ba_7Sn_3Se_{10.76(2)}Te_{2.24}$, respectively. Last, the possibility of partial ordering was explored in direct subgroups, including $Pna2_1$. Since no significant differences (i.e., no long range ordering) were found, and the residual factors did not improve, the final choice is the space group *Pnma*. Crystallographic details of the four data collections are summarized in Table 1, the atomic positions and isotropic displacement parameters of $Ba_7Sn_3Se_{13}$ in Table 2, and the occupancy factors of Q7 and Q8 of the three Te-containing examples in Table 3.

Electronic Structure Calculations. We performed self-consistent tight-binding first principle LMTO calculations (LMTO = linear muffin tin orbitals) using the atomic spheres approximation (ASA)[15,16] to study the impact of the Te substitution. In the LMTO approach, the density functional theory is used with the local density approximation (LDA) for the exchange correlation energy.[17] Three different models were calculated. To model $Ba_7Sn_3Se_{13}$, the data were taken from the X-ray structure refinements on $Ba_7Sn_3Se_{13}$, as listed in Tables 1 and 2. We used the structural data from the $Ba_7Sn_3Se_{10.76(2)}Te_{2.24}$ refinements first with six Te atoms on Q7 and three Te atoms on Q8, yielding the formula $Ba_7Sn_3Se_{10.75}Te_{2.25}$ in the space group *Pm* (and the same unit cell as before). Second, we assigned Te atoms to all Q7 and Q8 sites, retaining the symmetry of $Ba_7Sn_3Se_{13}$, yielding the hypothetical formula $Ba_7Sn_3Se_{10}Te_3$. The following wave functions were used: for Ba, 6s,6p (included via the downfolding technique),[18] 5d, and 4f; for Sn and Te, 5s, 5p, 5d (downfolded), and 4f (downfolded); and for Se, 4s, 4p, and 3d (downfolded). The integrations in k space (252 independent k points for $Ba_7Sn_3Se_{13}$) were performed by an improved tetrahedron method.[19] Integrated COHP values of selected Q−Q interactions were extracted from the energy-partitioning crystal orbital Hamilton

Table 2. Atomic Positions and Isotropic Displacement Parameters for $Ba_7Sn_3Se_{13}$

atom	site	X	y	z	U_{eq} (Å^2)
Ba1	8d	0.18699(5)	0.53175(2)	0.38011(7)	0.0168(1)
Ba2	8d	0.34417(7)	0.65542(3)	0.8974(1)	0.0354(2)
Ba3	4c	0.14456(7)	3/4	0.6050(1)	0.0209(2)
Ba4	8d	0.97853(5)	0.65762(3)	0.09313(8)	0.0232(2)
Sn1	4c	0.25902(7)	3/4	0.18937(1)	0.0147(2)
Sn2	8d	0.04761(5)	0.55118(3)	0.80279(8)	0.0137(1)
Se1	4c	0.9541(1)	3/4	0.3607(2)	0.0187(3)
Se2	8d	0.14225(8)	0.42702(4)	0.1412(1)	0.0174(2)
Se3	8d	0.16491(8)	0.57082(4)	0.0139(1)	0.0189(2)
Se4	4c	0.1487(1)	3/4	0.9648(2)	0.0175(3)
Se5	8d	0.21935(9)	0.66741(4)	0.3289(1)	0.0222(2)
Se6	8d	0.0887(1)	0.62155(4)	0.6155(1)	0.0257(3)
Se7	8d	0.07823(8)	0.46095(4)	0.68725(12)	0.0174(2)
Se8	4c	0.89553(13)	3/4	0.8240(2)	0.0283(4)

Table 3. Occupancies of the Q7 and Q8 Sites for $Ba_7Sn_3Se_{13-\delta}Te_\delta$

compound	% Se on Q7	% Se on Q8
$Ba_7Sn_3Se_{11.9}Te_{1.1}$	59.6(8)	70.5(11)
$Ba_7Sn_3Se_{11.2}Te_{1.8}$	37.8(5)	48.7(7)
$Ba_7Sn_3Se_{10.8}Te_{2.2}$	23.3(6)	28.9(9)

(13) *SAINT*; Version 4 ed.; Siemens Analytical X-ray Instruments Inc.: Madison, WI., 1995.
(14) Sheldrick, G. M. *SHELXTL*; Version 5.12 ed.; Siemens Analytical X-ray Systems: Madison, WI., 1995.
(15) Andersen, O. K. *Phys. Rev. B* **1975**, *12*, 3060−3083.
(16) Skriver, H. L. *The LMTO Method*; Springer: Berlin, Germany, 1984.
(17) Hedin, L.; Lundqvist, B. I. *J. Phys. C* **1971**, *4*, 2064−2083.
(18) Lambrecht, W. R. L.; Andersen, O. K. *Phys. Rev. B* **1986**, *34*, 2439−2449.
(19) Blöchl, P. E.; Jepsen, O.; Andersen, O. K. *Phys. Rev. B* **1994**, *49*, 16223−16233.

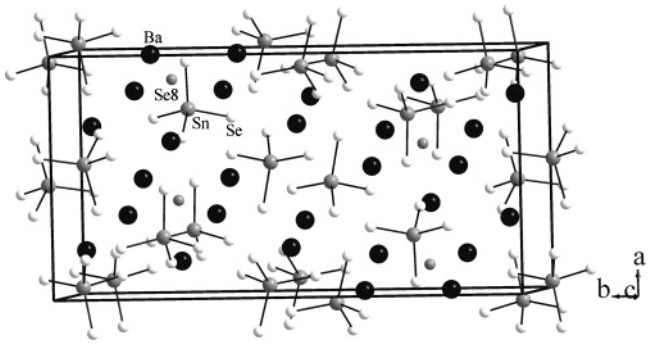

Figure 1. Projection of the $Ba_7Sn_3Se_{13}$ structure along the *c* axis. Ba−Se contacts are omitted for clarity.

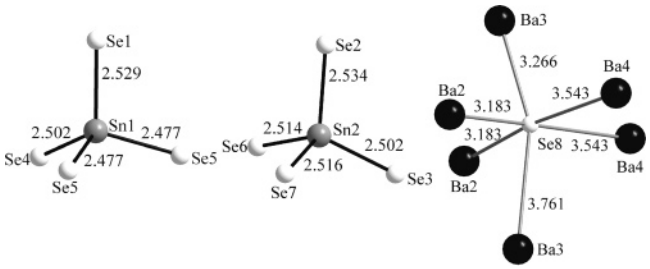

Figure 2. $SnSe_4$ tetrahedra and $Se8Ba_6$ "octahedron" (right) of $Ba_7Sn_3Se_{13}$. Bond distances are given in Å.

population scheme[20] to gain information about the bond strengths, comparable to the longer established Mulliken overlap populations[21] deduced from the crystal orbital overlap populations.[22]

Results and Discussion

Crystal Structures. The crystal structure of $Ba_7Sn_3Se_{13}$ is shown in Figure 1, wherein the Ba−Se bonds are omitted for clarity. This projection reveals two isolated $SnSe_4$ tetrahedra as well as an Se atom (Se8) not connected to any Sn atom, hence an isolated Se atom.

Unlike in the structure of Ba_2SnSe_5,[23] thus far the only other Ba Sn selenide, the Ba^{2+} cations are not stacked in channels in any direction. Moreover, the Ba cations in $Ba_7Sn_3Se_{13}$ are surrounded by six Se atoms in case of Ba2, eight (Ba4) and nine (Ba1, Ba3), while all Ba atoms of Ba_2SnSe_5 are coordinated by nine Se atoms. Qualitatively, this difference may be understood based on the higher Se/Ba ratio of 5:2 = 2.5 in Ba_2SnSe_5, as compared to 13:7 = 1.86 in $Ba_7Sn_3Se_{13}$. The Ba−Se coordination spheres in $Ba_7Sn_3Se_{13}$ are all quite irregular and may be described as (distorted) monocapped $Ba1Se_9$ and $Ba3Se_9$ square antiprisms, a bicapped trigonal $Ba4Se_8$ prism, and a $Ba2Se_6$ octahedron, with Ba−Se distances encompassing the wide range between 3.13 and 3.76 Å. The corresponding values in Ba_2SnSe_5 are 3.24−3.70 Å.

The $SnSe_4$ tetrahedra, on the other hand, are almost regular (Figure 2), with Sn−Se bonds between 2.48 and 2.53 Å (Table 4) and Se−Sn−Se bond angles ranging from 107 to 114°. These values compare well with those from the $SnSe_4$ tetrahedra of Ba_2SnSe_5 (e.g., distances between 2.51 and 2.58 Å). The bond lengths are typical for $Sn^{IV}Se_4$ tetrahedra, as also found in, for example, the isolated tetrahedra of K_4SnSe_4 (2.49−2.53 Å)[24] and $BaCu_2SnSe_4$ (2.52−2.55 Å).[25]

Table 4. Sn−Q Distances [Å] for $Ba_7Sn_3Se_{13-\delta}Te_\delta$

bond	$Ba_7Sn_3Se_{13}$	$Ba_7Sn_3Se_{11.9}Te_{1.1}$	$Ba_7Sn_3Se_{11.2}Te_{1.8}$	$Ba_7Sn_3Se_{10.8}Te_{2.2}$
Sn1−Se5 2	2.477(1)	2.470(1)	2.4759(5)	2.4839(7)
Sn1−Se4	2.502(2)	2.514(1)	2.5172(8)	2.515(1)
Sn1−Se1	2.529(2)	2.534(2)	2.5416(8)	2.543(1)
Sn2−Se3	2.502(1)	2.509(1)	2.5122(6)	2.5113(8)
Sn2−Se6	2.514(1)	2.512(1)	2.5140(6)	2.5155(8)
Sn2−Se2	2.534(1)	2.527(1)	2.5359(5)	2.5416(8)
Sn2−Q7	2.516(1)	2.624(1)	2.6744(5)	2.7007(6)
Q7−Sn2	2.516(1)	2.624(1)	2.6744(5)	2.7007(6)
Q7−Ba1	3.442(1)	3.500(1)	3.5283(5)	3.5433(6)
Q7−Ba1	3.485(1)	3.510(1)	3.5329(5)	3.5441(6)
Q7−Ba1	3.610(1)	3.651(1)	3.6727(5)	3.6839(6)
Q7−Ba4	3.651(1)	3.709(1)	3.7128(5)	3.7139(6)
Q8−Ba2 2	3.183(2)	3.304(1)	3.3476(5)	3.3805(7)
Q8−Ba3	3.265(2)	3.333(2)	3.3841(7)	3.4159(9)
Q8−Ba4 2	3.543(2)	3.466(1)	3.4865(5)	3.5074(7)
Q8−Ba3	3.762(2)	3.760(2)	3.7503(7)	3.7352(9)

It is the coordination sphere of the Se8 atom that makes this compound stand out in the series of alkaline/alkaline earth Sn selenides, as it forms no covalent Sn−Se bond. Instead, it is surrounded by six Ba atoms forming a distorted octahedron (right part of Figure 2), with Ba−Se distances between 3.18 and 3.76 Å. Additionally, Se8 participates in one of the shortest Se−Se distances of $Ba_7Sn_3Se_{13}$, namely, 3.48 Å to Se4—the shortest is the Se5−Se6 contact of 3.32 Å. Similar situations occur in $NaBa_6Cu_3Te_{14}$, with one of the Te atoms bonded only to Ba atoms,[26] and in Ba_2CoCl_6, where one Cl atom is bonded exclusively to Ba atoms.[27] While it is obvious from the Sn/Se ratio of 3:13 (<1:4) that not all Se atoms can bond to Sn, if only $SnSe_4$ tetrahedra are present, an alternative to the here observed scenario would be an increase of the Sn coordination number beyond four. The latter occurs in Ba_2SnSe_5, where one Sn atom is octahedrally coordinated by six Se atoms.

The assignment of oxidation states in $Ba_7Sn_3Se_{13}$ is straightforward, as the Sn−Se coordination is typical for Sn^{IV}, and no Se−Se bonds occur. This then results in the balanced formula $(Ba^{II})_7(Sn^{IV})_3(Se^{II-})_{13}$. To indicate the presence of $SnSe_4$ tetrahedra and isolated Se atoms in $Ba_7Sn_3Se_{13}$, we rewrite it as $(Ba^{II})_7(SnSe_4{}^{IV-})_3Se^{II-}$. It is intriguing that such a compound is thermodynamically preferred over three Ba_2SnSe_4 and one BaSe. We note that Ba_2SnSe_4 might not exist, as it has not been reported yet, and our attempts to synthesize it have failed so far. On the other hand, two Ba_2SnS_4 modifications[11,12] are known, and no Ba_2SnTe_4 was observed. As each of the Ba atoms of the two Ba_2SnS_4 modifications comprises only six or seven S contacts, we hypothesize that the tendency to higher coordination numbers in the Se case favors the existence of the complex structure of $Ba_7Sn_3Se_{13}$ with up to nine Ba−Se bonds per Ba^{2+}.

(20) Dronskowski, R.; Blöchl, P. E. *J. Phys. Chem.* **1993**, *97*, 8617−8624.
(21) Mulliken, R. S. *J. Chem. Phys.* **1955**, *23*, 2343−2346.
(22) Hughbanks, T.; Hoffmann, R. *J. Am. Chem. Soc.* **1983**, *105*, 3528−3537.
(23) Assoud, A.; Soheilnia, N.; Kleinke, H. *J. Solid State Chem.* **2005**, *178*, 1087−1093.
(24) Klepp, K. O. *Z. Naturforsch.* **1992**, *47b*, 411−417.
(25) Assoud, A.; Soheilnia, N.; Kleinke, H. *Chem. Mater.* **2005**, *17*, 2255−2261.
(26) Zhang, X.; Schindler, J. L.; Hogan, T.; Albritton-Thomas, J.; Kannewurf, C. R.; Kanatzidis, M. G. *Angew. Chem., Int. Ed. Engl.* **1995**, *34*, 68−71.
(27) Assoud, A.; Wickleder, C.; Meyer, G. *Z. Anorg. Allg. Chem.* **2000**, *626*, 2103−2106.

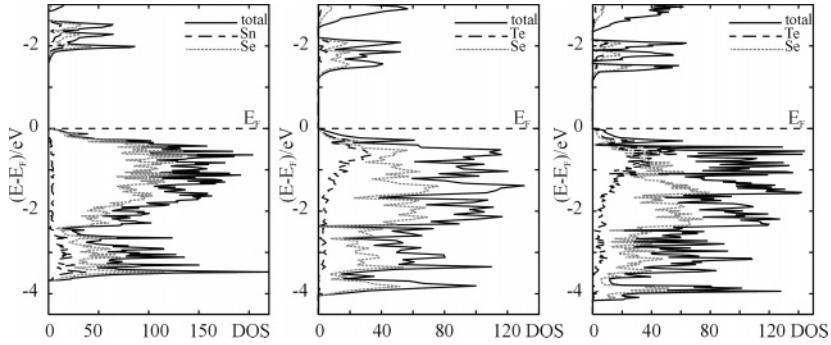

Figure 3. Densities of states (DOS) of $Ba_7Sn_3Se_{13}$ (left), $Ba_7Sn_3Se_{10.75}Te_{2.25}$ (center) and $Ba_7Sn_3Se_{10}Te_3$ (right). The dashed horizontal lines indicate the Fermi energy, E_F.

Our systematic attempts to replace Se atoms with Te atoms in $Ba_7Sn_3Se_{13}$ revealed the phase range of $Ba_7Sn_3Se_{13-\delta}Te_\delta$ to be within $0 \le \delta \le 2.24(2)$. Hence, we conclude that the pure telluride $Ba_7Sn_3Te_{13}$ is not likely to exist. The Te atoms evidently prefer two sites in $Ba_7Sn_3Se_{13-\delta}Te_\delta$, namely, the Q7 and Q8 sites (called Se7 and Se8 in the selenide). These sites accommodate each more than 70% Te at the Te-rich border of the phase range, while the other Se sites remain Te free. Q8 is the site without Sn-Q contacts, and upon Te incorporation, the $Q8Ba_6$ octahedron becomes increasingly more regular: the two shortest Q8−Ba bonds of 3.18 Å increase most significantly up to 3.38 Å, while the three longest of 3.54−3.76 Å actually decrease to 3.51−3.74 Å. This may be compared to the six Te−Ba distances of 3.42 Å in BaTe (NaCl type) and the six Te−Ba distances in $NaBa_6Cu_3Te_{14}$ of 3.49 Å.[26] Furthermore, the Q8−Se4 distance increases as well to 3.55−3.59 Å in the three selenide−tellurides studied.

The Q7 atom stands out, as it exhibits the longest Q7−Ba distances in $Ba_7Sn_3Se_{13}$, starting at 3.44 Å, and is one of the few Q sites with a coordination number of five. The Q7−Sn2 bond increases rapidly with increasing Te content (i.e., by 0.11 Å in $Ba_7Sn_3Se_{11.9}Te_{1.1}$), while the other Q−Sn distances remain virtually unchanged, with a maximum increase of 0.01 Å (Table 4). A comparison of the SnQ_4 tetrahedra of Ba_2SnSe_5 (2.51−2.58 Å) and the two modifications of Ba_2SnTe_5 (2.72−2.82 Å)[9,28] indicates that Sn^{IV}−Te bonds of 4-fold coordinated Sn atoms typically are about 0.2 Å longer than Sn^{IV}−Se bonds.

Electronic Structures. The computed densities of states of $Ba_7Sn_3Se_{13}$ (left part of Figure 3) support the previously mentioned assignment of oxidation states, for the only filled valence orbitals are the Se-s states (below the energy window shown) and Se-p states (located between −3.7 eV and the Fermi level, E_F, at 0 eV). The Sn-s contributions (of antibonding Sn−Se character) start well above the Se-p based peak, separated by a band gap of 1.6 eV. These values are significantly different in the $Ba_7Sn_3Se_{10.75}Te_{2.25}$ model, where the chalcogen-p states start at −4.1 eV, and the band gap is 1.2 eV (middle part of Figure 3). The chalcogen peak continuously widens to 4.2 eV, and the band gap decreases to 1.1 eV in the $Ba_7Sn_3Se_{10}Te_3$ model.

Both trends (i.e., that the band gap decreases and that the width of the chalcogen-p band increases with increasing Te content) are caused by the higher lying Te-p states, as compared to Se-p. The projections of the Te states onto the DOS confirm this, revealing the maximum Te-p contributions at the upper region of the chalcogen-p peak. Experimentally, we observed the color red for $Ba_7Sn_3Se_{13}$, which turns increasingly dark with increasing Te content (e.g., to almost black for $Ba_7Sn_3Se_{10.76(2)}Te_{2.24}$). Since these colors correspond to band gaps between 2 eV (red) and 1.7 eV (almost black),[29] the calculations yielded the correct trend, but the calculated band gaps turned out to be too small by about 20−30%. We observed a similar difference of 25% in the case of the red semiconductor $Ba_4LaSbGe_3Se_{13}$,[30] noting that it is the calculation method that often results in too small band gaps.[31,32]

The polyselenide Ba_2SnSe_5 exhibits a significantly smaller band gap, both computed (1.2 vs 1.6 eV) as well as evident from the color (dark brown vs red). Two main reasons can be identified for this difference. First, the filled Se-p peak is wider in Ba_2SnSe_5 (4.5 vs 3.7 eV), and second, empty Se−Se antibonding states appear only in Ba_2SnSe_5 between the E_F and the Sn-s states.

We utilized the crystal orbital Hamilton population (COHP) to investigate the peculiar intermediate Q−Q contacts <3.6 Å. These are (mostly weakly) antibonding, in accord with the assigned oxidation states of −2. For example, the integrated COHP values of the Se5−Se6 (3.34 Å) and Se4−Te8 (3.59 Å) interactions of the model $Ba_7Sn_3Se_{10}Te_3$ are +0.08 and +0.21 eV/bond, respectively. The latter significantly antibonding value may be the reason the Q8 site cannot be fully occupied by Te atoms, for Se−Se distances of that length would be nonbonding.

Conclusion

The new selenide $Ba_7Sn_3Se_{13}$ is a red semiconductor that forms its own structure type with isolated $Sn^{IV}Se_4$ tetrahedra and Se atoms. The latter is unique in this class of seleno−stannates. Up to 2.24(2) Te atoms may replace the Se atoms of $Ba_7Sn_3Se_{13}$, resulting in a calculated band gap decrease

(28) Li, J.; Liszewski, Y. Y.; MacAdams, L. A. *Chem. Mater.* **1996**, *8*, 598−600.
(29) Nassau, K. *The Physics and Chemistry of Color*; 2nd ed.; John Wiley & Sons: New York City, NY, 2001.
(30) Assoud, A.; Soheilnia, N.; Kleinke, H. *J. Solid State Chem.* **2004**, *177*, 2249−2254.
(31) Yanagi, H.; Inoue, S.-I.; Ueda, K.; Kawazoe, H. *J. Appl. Phys.* **2000**, *88*, 4159−4163.
(32) Tampier, M.; Johrendt, D. *Z. Anorg. Allg. Chem.* **2001**, *627*, 312−320.

from 1.6 to 1.2 eV. The change of color from red to almost black proves this calculated trend to be correct; however, the calculated gaps should be 20−30% larger, according to the observed colors. Thus, for this or a related material to be of interest for the thermoelectric energy conversion, one would have to go to the respective telluride or add polychalcogenide groups since, for example, Ba_2SnSe_5 exhibits a significantly smaller gap than $Ba_7Sn_3Se_{13}$ because of the presence of empty antibonding Se−Se states slightly above the Fermi level.

Acknowledgment. Financial support from NSERC, CFI, OIT (Ontario Distinguished Researcher Award for H.K.), the Province of Ontario (Premier's Research Excellence Award for H.K.) and the Canada Research Chair program (CRC for H.K.) is appreciated.

Supporting Information Available: Four X-ray crystallographic files (CIF). This material is available free of charge via the Internet at http://pubs.acs.org.

CM050787Y